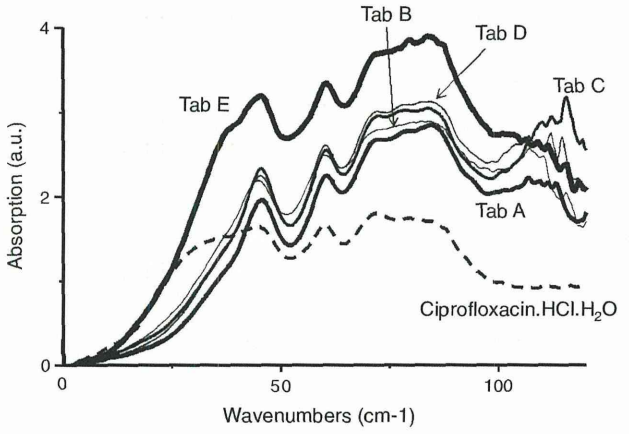

Fig. 1 Terahertz spectra of ciprofloxacin hydrochloride monohydrate (*broken line*) and five different commercial tablets (*solid lines*)

that tablets A, B, C, and D are all consistent with each other and with the spectra of CPFX·HCl·H_2O (broken line). Although the spectral feature of tablet E was different from those of the other tablets, the spectral feature that is lower wavenumber than 40 cm^{-1} was similar to that of CPFX·HCl·H_2O. According to the enclosed documents for the products, CPFX·HCl·H_2O is the active ingredient in each product. These results suggest that terahertz spectroscopy can be used to identify API in tablets.

Figure 2 shows the second derivative of terahertz absorption spectra obtained from the commercial tablets. The peaks at 60 and 46 cm^{-1} were observed in all of the tablets. The peaks at 88, 85, 84, 79, and 71 cm^{-1} detected in tablet A may be water vapor lines.

Table 1 shows the ingredients listed in the manufacturer's product literature. This shows that similar ingredients are used for all tablet formulations. Unfortunately, the literature does not disclose the percentage content of each ingredient.

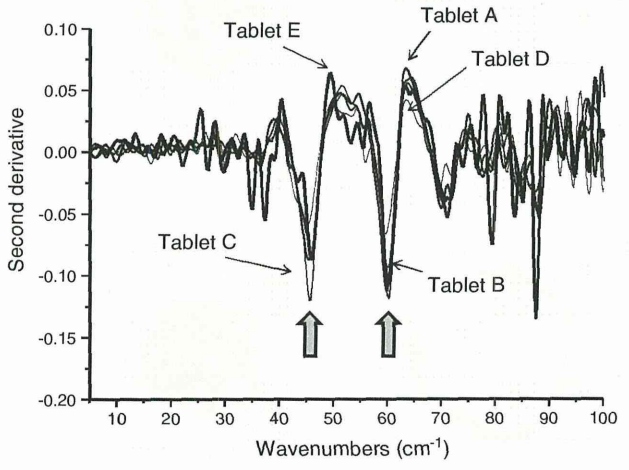

Fig. 2 Second derivative terahertz spectra of the five different commercial tablets

Analysis of Quality Attributes of Tablets Using Terahertz Imaging System

Density Distribution of Film-Coated Tablets

Figure 3 shows the distribution maps of the reflected peak intensities from the surface (A) and 0.26 mm depth (B) of the tablets obtained from each of the measured commercial tablets, respectively. Tablets A and B each have a homogeneous distribution of the peak reflected strength from the surface of the coating, while tablets C and D each have a heterogeneous distribution. As discussed previously, Ho et al. [17] correlated the intensity of reflection to the refractive index of the coating from the equation

$$R = \frac{(n-1)}{(n+1)}$$

where R is the intensity of the reflection and n is the terahertz refractive index of the material. The intensity of reflection from each tablet measured is shown in Fig. 3; these values are labeled with the letter A. They indicate differences between each of the tablets. From the equation described above, we can relate the R to the terahertz refractive index of the coating. This is an indication of a change in the density of the coating. During scale-up of a sustained-release coating product, Ho et al. [19] also showed that similar changes in the density of the coating (or in the intensity of reflection from the tablet) can affect product performance. In the case of the tablets studied in this paper, the coating prevents the decomposition of API by light exposure. So, we do not expect the coating to affect the tablets' dissolution performance. However, this study will provide the sensitivity needed for terahertz measurements against this parameter. We also observe a variation in the intensity of reflection across the surfaces of tablets A and B. This may suggest regions of defective coating or changes in local density on the tablets.

A terahertz dataset allows the experimenter to generate maps at different depths within a tablet without sectioning the tablet. Image B in Fig. 3 shows the distribution of relative refractive indices changing from the tablet surface to a depth of 260 μm. In the images of tablets A and D, the changes in refraction of terahertz pulsed wave by penetrating of component which has different refractive indices are larger at the centers of the tablets than at their outer circles. And tablet B shows comparatively large changes in refraction of terahertz pulsed wave through the wider area of the tablet. In the image obtained from tablet C, small areas having comparatively small changes in refraction of terahertz pulsed wave appear in the center of the tablet. Meanwhile, the edge of the tablet shows larger change in

Table 1 Ingredients contained in each of five commercial tablets

Tablet A		
Corn starch	Magnesium stearate	Cellulose
Titanium dioxide	Hydroxypropylmethylcellulose (HPMC)	
Carboxymethylstarch soduim	Povidon	Silicate unhydrate
Tablet B		
Corn starch	Cellulose	Magnesium stearate
Titanium dioxide	HPMC	
Macrogol	Crosspovidon	Silicate unhydrate
Tablet C		
Corn starch	Crystallized cellulose	Magnesium stearate
Titanium dioxide	HPMC	
Macrogol 6000	Light anhydrous silicic acid	Tarc
Carboxymethylstarch soduim	Lactose	Carnauba wax
Tablet D		
Corn starch	Hydroxypropylcellulose	Magnesium stearate
Titanium dioxide	HPMC	
Macrogol	Carboxymethylstarch sodium	Citric acid hydrate
Tablet E		
Corn starch	Crystallized cellulose	Magnesium stearate
Titanium dioxide	HPMC 2910	
Macrogol 4000	Crosspovidon	Light anhydrous silicic acid

refraction. These observations indicate that features of a tablet's physical state resulting from the manufacturing process, such as the uneven distribution of granule sizes or the uneven penetration of compression force in a mortar, will change the density of tablet components.

In-Depth Terahertz Images

The depth (B-scan) terahertz images obtained from commercial tablets A–D are shown in Fig. 4. These tablets each have a coating thickness of approximately 100 μm. The left

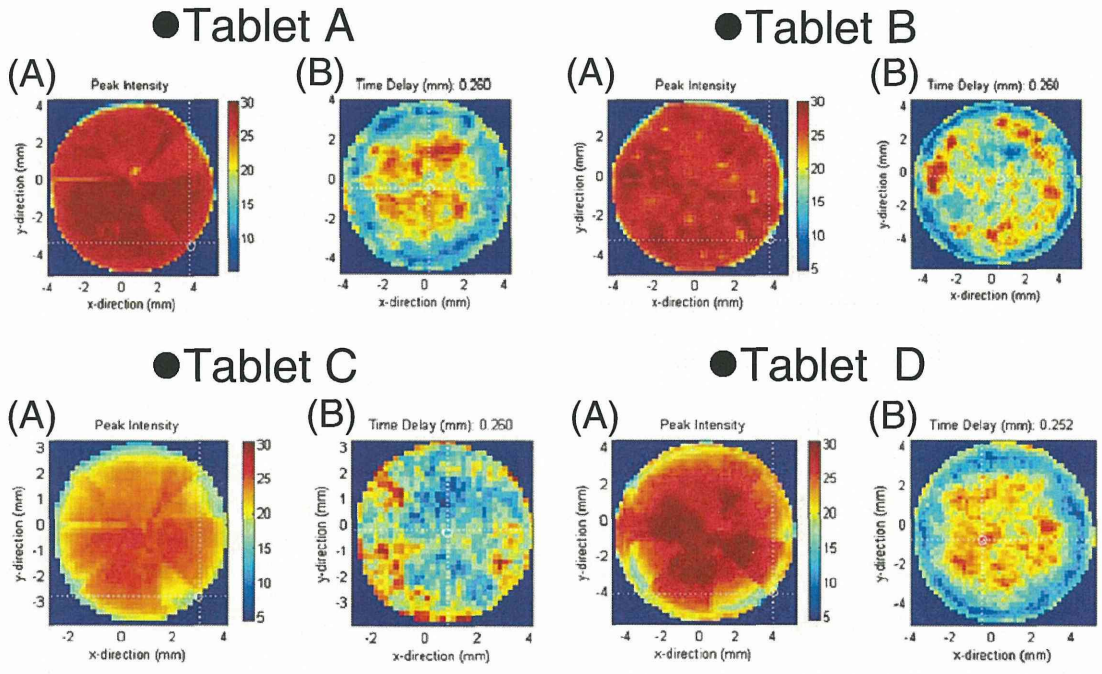

Fig. 3 Terahertz images of four different commercial tablets (**a** surface area and **b** at 0.26 mm depth from the surface)

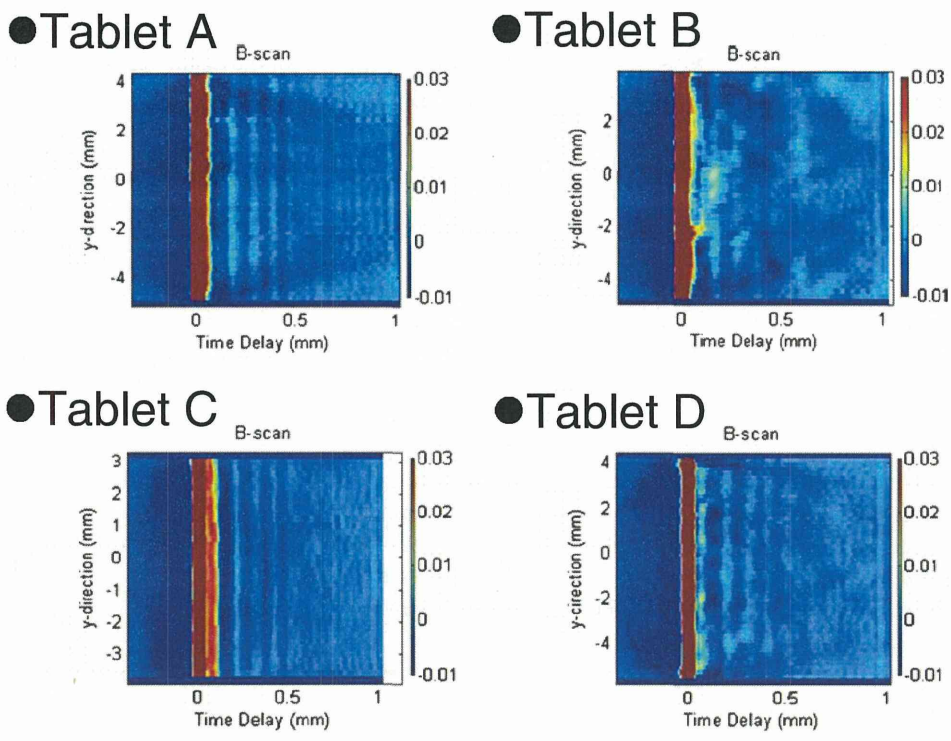

Fig. 4 Depth (*B-Scan*) terahertz images of four different commercial tablets (the area to the right of each brown line represents the inside of a tablet)

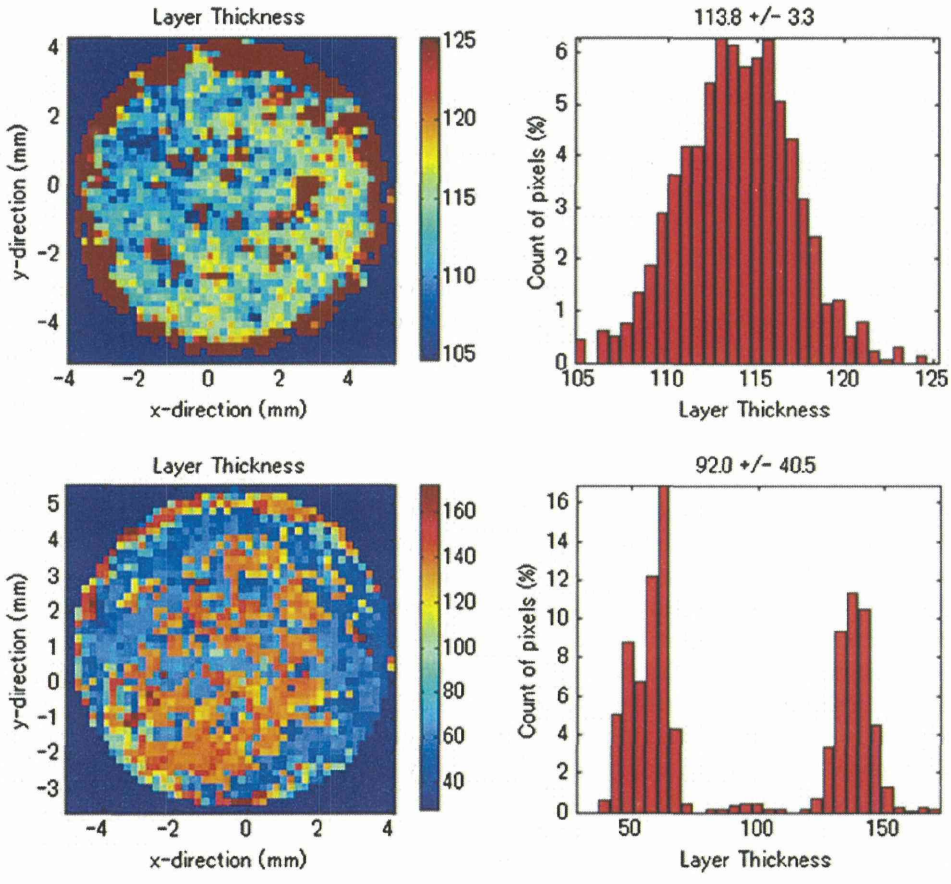

Fig. 5 Distribution of coating thickness (*left*) and histograms (*right*) (*upper images*, *Tablet A*; *lower images*, *Tablet D*)

and right sides of the brown line represent air and the inside of the tablet, respectively. The echoes showing several layers formed by compression are observed. Definite layers up to 1 mm depth and up to 0.5 mm depth appear in Tablets A and C, respectively. The indistinct echoes can be seen in Tablet D. On the other hand, indistinct but layer-like echoes are observed in Tablet B. Those observations suggest that unevenly penetrated compression force into the tablet. Further study is necessary to explain the details of these results. However, features of the pre-compression state, such as the particle size distribution of components in a mortar, would be affected by the penetration of compression force in the tablet compaction process. This physical property would be represented as echoes in depth terahertz images. Thus, a depth (B-scan) terahertz image would provide physical information about the effects of the manufacturing process on the tablet's state and also would sensitively detect changes in manufacturing quality.

Distribution of Coating Thickness

Figure 5 shows the distributions of coating thicknesses obtained from Tablets A and D. A histogram of the coating thickness of each tablet is shown at the right side of this figure. In the case of tablet A, the coating thickness was between 105 and 125 μm, a relatively narrow range of 20 μm. The coating thickness on the outer circuit of each tablet image shows a tendency toward relative thickness, and that on the center shows the opposite tendency. In the case of Tablet D, two peaks in the coating thickness range (40 to 70 and 120 to 150 μm) appear. Moreover, the thin and thick layers are irregularly distributed in the image. This observation definitely indicates that the coating property depends on the coating process. These results suggest that an inappropriate coating process was performed for tablet D.

Conclusions

A tablet containing relatively large amounts of API (from 75.1 to 82.3 %) would be detected qualitatively by comparison against the characteristic terahertz waveform of API. Terahertz imaging can reveal coating thicknesses and their distributions, the densities of components by compression, and hollows on a tablet surface based on the detection of the delayed reflection of terahertz pulses. Detection of the coating state and changes in the physical state, such as density distribution inside a tablet, would contribute not only to the identification of manufacturing quality but also to qualitative confirmation of commercial tablets including fake (counterfeit) and/or defective products. The TPS and imaging techniques will be useful as nondestructive analytical tools for the quality control of commercial tablets.

Acknowledgments This study was supported in part by a research grant from the Ministry of Health, Labour, and Welfare of Japan (H20-iyaku-ippan-004). The authors would like to thank Mr. Tsuyoshi Miura, Mr. Daisuke Sasakura, and Mr. Tomoyuki Matsubara (Bruker Optics K.K., Japan) for their kind assistance.

References

1. Korter TM, et al. Terahertz spectroscopy of solid serine and cysteine. Chem Phys Lett. 2006;418:65–70.
2. Day GM, et al. Understanding the influence of polymorphism on phonon spectra: lattice dynamics calculations and terahertz spectroscopy of carbamazepine. J Phys Chem B. 2006;110:447–56.
3. Allis DG, et al. Solid-state modeling of the terahertz spectrum of the high explosive HMX. J Phys Chem A. 2006;110:1951–9.
4. Saito S, et al. Terahertz vibrational modes of crystalline salicylic acid by numerical model using periodic density functional theory. Jpn J Appl Phys Part 1-Regul Pap Brief Commun Rev Pap. 2006;45:4170–5.
5. Saito S, et al. Terahertz phonon modes of an intermolecular network of hydrogen bonds in an anhydrous beta-D-glucopyranose crystal. Chem Phys Lett. 2006;423:439–44.
6. Allis DG, et al. Theoretical analysis of the terahertz spectrum of the high explosive PETN. Chem Phys Chem. 2006;7:2398–408.
7. Taday PF, et al. Using terahertz pulse spectroscopy to study the crystalline structure of a drug: a case study of the polymorphs of ranitidine hydrochloride. J Pharm Sci. 2003;92:831–8.
8. Walther M, et al. Noncovalent intermolecular forces in polycrystalline and amorphous saccharides in the far infrared. Chem Phys. 2003;288:261–8.
9. Strachan CJ, et al. Using terahertz pulsed spectroscopy to study crystallinity of pharmaceutical materials. Chem Phys Lett. 2004;390:20–4.
10. Zeitler JA, et al. Characterization of temperature induced phase transitions in the five polymorphic forms of sulfathiazole by terahertz pulsed spectroscopy and differential scanning calorimetry. J Pharm Sci. 2006;95:2486–98.
11. Zeitler JA, et al. Temperature dependent terahertz pulsed spectroscopy of carbamazepine. Thermochimica Acta. 2005;436:70–6.
12. Strachan CJ, et al. Using terahertz pulsed spectroscopy to quantify pharmaceutical polymorphism and crystallinity. J Pharm Sci. 2005;94:837–46.
13. Zeitler JA, et al. Relaxation and crystallization of amorphous carbamazepine studied by terahertz pulsed spectroscopy. J Pharm Sci. 2007;96:2703–9.
14. Kogermann K, et al. Investigating dehydration from compacts using terahertz pulsed, Raman, and near-infrared spectroscopy. Appl Spectrosc. 2007;61:1265–74.
15. Zeitler JA, et al. Characterization of drug hydrate systems and dehydration processes using terahertz pulsed spectroscopy. Int J of Pharmaceutics. 2007;334:78–84.
16. Liu H-B, et al. Characterization of anhydrous and hydrated pharmaceutical materials with THz time-domain spectroscopy. J Pharm Sci. 2007;96:927–34.

17. Ho L, et al. Analysis of sustained-release tablet film coats using terahertz pulsed imaging. J Control Release. 2007;119:253–61.
18. Ho L, et al. Applications of terahertz pulsed imaging to sustained-release tablet film coating quality assessment and dissolution performance. J Control Release. 2008;127:79–87.
19. Ho L, et al. Terahertz pulsed imaging as an analytical tool for sustained-release tablet film coating. Eur J Pharm Biopharm. 2009;71:117–23.
20. Fitzgerald AJ, et al. Nondestructive analysis of tablet coating thicknesses using terahertz pulsed imaging. J Pharm Sci. 2005;94:177–83.
21. Zeitler JA, et al. Analysis of coating structures and interfaces in solid oral dosage forms by three dimensional terahertz pulsed imaging. J Pharm Sci. 2007;96:330–40.
22. Sakamoto T, et al. Detection of tulobuterol crystal in transdermal patches using terahertz pulsed spectroscopy and imaging. Pharmazie. 2009;64:361–5.